

Modified Dual-Switch Boost DC–DC Converter for Fuel Cell Vehicles

Mr. Althaf P K¹, Prof. Beena M Varghese², Dr. Jisha Kuruvila³, Dr. Sija Gopinathan⁴, Dr. Siny Paul⁵,
Dr. Reenu George⁶

¹PG Scholar Dept of Electrical & Electronics Engg, Mar Athanasius College of Engineering
Kothamangalam, Kerala, India

^{2,3,4,5,6}Dept of Electrical & Electronics Engg, Mar Athanasius College of Engineering Kothamangalam,
Kerala, India

Abstract—A DC-DC converter designed for fuel cell vehicle applications must deliver high voltage gain, low voltage stress on components, compact size, and high efficiency. Traditional converter topologies such as two-level, three-level, and cascaded boost converters often fall short in fulfilling these criteria. To address these limitations, a novel non-isolated converter incorporating a switched-capacitor network is introduced. This design achieves a significant voltage gain, supports a wide input voltage range, maintains low voltage stress across the components, and offers a common ground configuration. The proposed high-gain converter ensures continuous input current, reduced voltage stress, and a minimal component count, all while maintaining a grounded architecture. A detailed steady-state analysis is carried out in continuous conduction mode (CCM), and its performance is compared with other state-of-the-art converter designs. Simulation studies, performed using MATLAB/SIMULINK, confirm the theoretical predictions and demonstrate the efficiency and effectiveness of the proposed topology. For experimental validation, a hardware prototype is built using the TMS320F28027F microcontroller. With an input voltage of 2V, the prototype successfully delivers an output of 9V, achieving a voltage gain of 4.5. Under rated operating conditions, the converter attains a peak efficiency of 93.1%

Index Terms—Boost Converter, Fuel cell vehicles, Gain, Efficiency.

I. INTRODUCTION

The growth of the transportation sector significantly influences a nation's economic development. However, the widespread use of traditional fuel-powered vehicles leads to excessive consumption of

fossil fuels and contributes heavily to environmental degradation. As a result, global attention has shifted toward clean and sustainable energy solutions. One promising approach is the advancement of new energy vehicles, particularly fuel cell vehicles, which offer advantages such as zero emissions, minimal environmental impact, and high energy efficiency [3].

Although the conventional boost DC-DC converter remains popular in various applications due to its simple design and limited component count, it faces several limitations. The theoretical voltage gain of this converter is given by $1/(1-D)$, where D represents the duty cycle. However, in practice, parasitic elements within the components and circuitry limit the achievable gain [2]. Additionally, the high voltage stress across components demands the use of costly high-voltage-rated devices, which increases both the physical size and overall cost of the converter. Moreover, achieving high voltage gain requires operation at extreme duty cycles, which introduces severe diode reverse recovery issues and elevates power losses. These challenges render the traditional boost converter less suitable for use in fuel cell vehicle systems.

To overcome these limitations, alternative configurations such as cascaded boost converters have been considered. While they provide high voltage gain and a broad input voltage range, they compromise efficiency and power density due to increased component stress and complex circuitry. Similarly, three-level boost converters can alleviate voltage stress issues but do not significantly improve the voltage gain compared to the standard boost

converter.

One straightforward method to attain higher voltage gain involves cascading multiple boost converter stages—often referred to as cascade or quadratic boost converters. However, as the number of stages increases, so does the component count, leading to reduced efficiency, increased circuit complexity, and higher costs. To mitigate these issues, a single-switch quadratic converter configuration is typically used to lower the number of components. Nonetheless, this design results in higher conduction and switching losses since all cell currents are handled by a single switch.

To enhance power conversion efficiency under these conditions soft-switching techniques are adopted. In particular, Zero Voltage Switching (ZVS) is implemented to minimize switching losses. However, this requires the addition of auxiliary switches and a more sophisticated control strategy, introducing further complexity to the converter design.

A key advantage of the proposed converter is its common

ground configuration, which not only simplifies interfacing with control circuits and sensors but also minimizes electromagnetic interference (EMI). Moreover, the converter design achieves low input current ripple due to the dual-switch architecture combined with input-side inductance. This ripple minimization is especially beneficial for fuel cells, which are sensitive to high-frequency current disturbances.

Additionally, the incorporation of a voltage multiplier stage allows for gain expansion without significantly increasing the duty cycle, overcoming the limitations of converters operating in the extreme duty range (close to $D \rightarrow 1$). This ensures stable operation, reduced diode reverse recovery issues, and lower switching losses.

The performance of the modified converter is analyzed in both steady-state and small signal conditions, demonstrating its robustness across wide input voltage variations. Experimental validation using a laboratory prototype confirms the analytical findings. In summary, the proposed converter architecture presents a cost-effective, efficient, and scalable solution for high-gain DC–DC conversion in emerging electric and hydro gen fuel cell vehicles. Its design also holds promise for broader applications including portable energy systems,

renewable energy harvesting, and grid-connected distributed energy resources.

II. METHODOLOGY

The Modified Dual-Switch Boost DC-DC Converter architecture incorporates two main switches (S_1 and S_2), six diodes (D_1 through D_6), a single inductor (L), and five capacitors (C_1 to C_5). This configuration is designed to enhance voltage gain and reduce component stress while maintaining a relatively simple structure. The detailed topology of this converter is illustrated in Figure 3.6, which highlights the arrangement and interconnection of all the components involved.

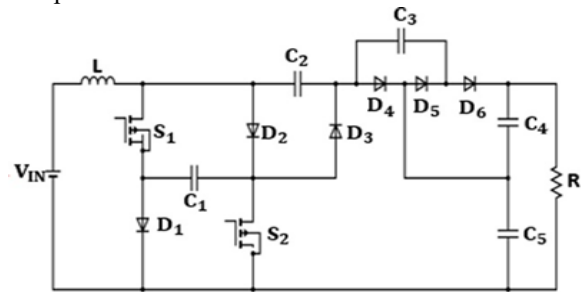


Fig. 1. Modified Dual-Switch Boost DC-DC Converter

A. Modes of Operation

The proposed boost converter operates primarily in two modes: Continuous Conduction Mode (CCM) and Continuous Bidirectional Conduction Mode (CBCM).

1) *Mode 1:* At time $t = t_0$, when switch S is activated and switches S_1 and S_2 are turned ON, the inductor L begins to charge. During this interval, diodes D_3 and D_5 are forward-biased, while diodes D_1 , D_2 , D_4 , and D_6 remain reverse-biased. Capacitors C_2 and C_3 are charged, whereas capacitors C_1 , C_4 , and C_5 discharge. The circuit operation corresponding to Mode 1 is illustrated in Figure?

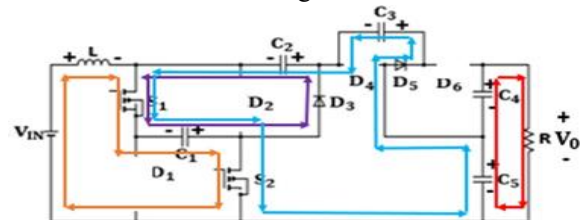


Fig. 2. Operating circuit of of Mode 1

2) *Mode 2*: At time $t = t_1$, when switch S is turned OFF and switches S_1 and S_2 are OFF, the inductor L discharges. During this period, diodes $D_1, D_2, D_4,$ and D_6 are forward-biased, while diodes D_3 and D_5 remain reverse-biased. Capacitors $C_1, C_4,$ and C_5 charge, whereas capacitors C_2 and C_3 discharge. The circuit operation corresponding to Mode 2 is illustrated in Figure?

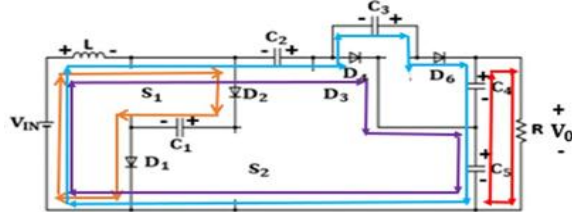


Fig. 3. Operating circuit of of Mode 2

Figure 4 illustrates the theoretical waveforms corresponding to Mode 1 and Mode 2.

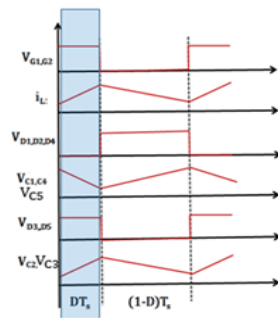


Fig. 4. Theoretical waveform

B. Design of Components

The input voltage is set to $V_{in} = 48$ V. The output power and output voltage are specified as $P_o = 100$ W and $V_o = 200$ V, respectively. The switching frequency is $f_s = 50$ kHz, which corresponds to a time period of $T_s = 1/f_s = 20 \mu s$. Load resistance can be found by the equation,

$$R_o = \frac{V_o^2}{P_o} = \frac{200^2}{100} = 400 \Omega \tag{1}$$

Voltage Gain,

$$M = \frac{V_o}{V_{in}} = \frac{4}{1-2D}, D = 0.02 \tag{2}$$

The inductors L is obtained from the following equations.

$$I_L = \frac{P}{V_{in}} = \frac{4 \cdot I_o}{1-2D} = \frac{4 \cdot 0.5}{1-2 \cdot 0.02} = 2.08A \tag{3}$$

$$L \geq \frac{4 \cdot I_o \cdot (1-D) \cdot D}{\Delta I \cdot L \cdot f_s (1-2D)} \geq 2mH \tag{4}$$

It is approximated to 2 mH. The values of the capacitors are determined using the following

equations.

$$C_1, C_2 \geq \frac{2 \cdot V_o \cdot D}{(1-2D) \cdot \Delta V_{C1} \cdot R \cdot f_s} \tag{5}$$

C_1 and C_2 is taken as 47 μF

$$C_3 \geq \frac{4 \cdot V_o \cdot D}{(1-2D) \cdot \Delta V_{C3} \cdot R \cdot f_s} \tag{6}$$

$$C_4 \geq \frac{D \cdot V_o}{R \cdot \Delta V_{C4} \cdot f_s} \tag{7}$$

$$C_5 \geq \frac{2 \cdot V_o \cdot (3+2D) \cdot D}{(1-2D) \cdot \Delta V_{C5} \cdot R \cdot f_s} \tag{8}$$

C_3, C_4 and C_5 are taken as 100 μF

III. SIMULATIONS AND RESULTS

The Modified Dual-Switch Boost DC-DC Converter is modeled and simulated using MATLAB/SIMULINK, utilizing the design parameters specified in Table 1. In this simulation, MOSFETs are employed as the switching devices, operating at a fixed switching frequency of 50 kHz. This simulation setup enables the evaluation of the converter’s performance under various conditions, ensuring accurate validation of its voltage gain, efficiency, and dynamic behavior. In the simulation, a

TABLE I

SIMULATION PARAMETERS OF MODIFIED DUAL-SWITCH BOOST DC-DC CONVERTER

Parameters	Specification
Input voltage V_{in}	48 V
Output voltage V_o	200 V
Inductor L	2000 μ H,5A
Capacitor C_1, C_2	47 μ F,150V
Capacitor C_3, C_4, C_5	100 μ F,250V
Switching frequency	50 kHz
Output load	400 Ω
Duty ratio	2 %

DC input voltage of 48 V was applied to the converter, and it successfully produced an output voltage of 200 V while supplying an output power of 100 W. The waveforms for the input voltage and current are shown in Figure 5, and the output voltage and current waveforms are presented in Figure 6.

Based on the input and output voltages, the voltage gain of the converter is calculated as:

$$\text{Voltage Gain} = \frac{V_{out}}{V_{in}} = \frac{200}{48} \approx 4.17 \tag{9}$$

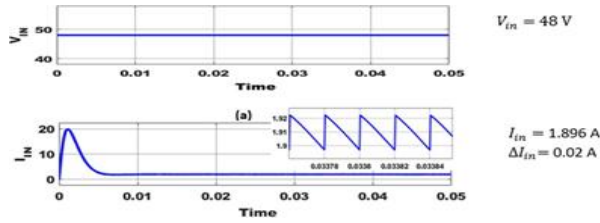


Fig. 5. (a) Input Voltage (V_{in}) and (b) Input Current (I_{in})

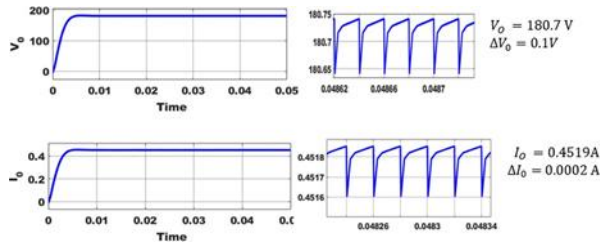


Fig. 6. (a) Output Voltage (V_o) and (b) Output Current (I_o)

Figures 7 and 8 illustrate the gate drive signals and the voltage stresses experienced by the switches in the converter circuit. The measured voltage stress across switch S1 is approximately 42.95V, while switch S2 experiences a slightly higher stress of around 49.25V.

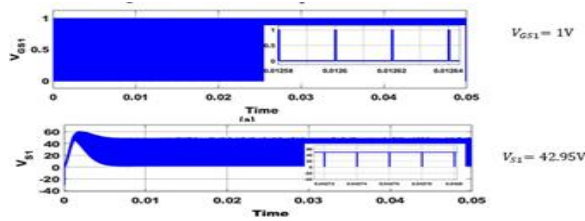


Fig. 7. Gate Pulse (V_{gs1}) and Voltage Stress (V_{s1}) of switch S1

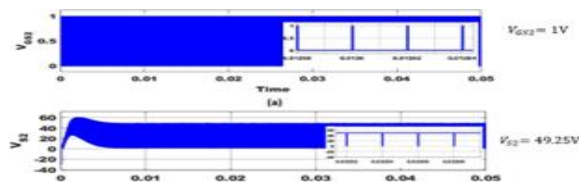


Fig. 8. Gate Pulse (V_{gs2}) and Voltage Stress (V_{s2}) of switch S2

The voltages across the capacitors are measured as $V_{C1} = 48.45$ V, $V_{C2} = 42.45$ V, $V_{C3} = 89.04$ V, $V_{C4} = 89.04$ V, and $V_{C5} = 91.7$ V, as illustrated in Fig. 8. Fig. 9 presents the current through the inductor L , showing that the filter inductance

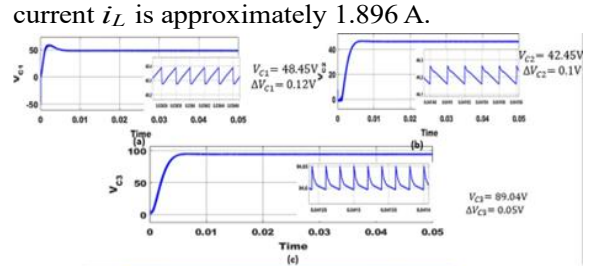


Fig. 9. Voltage across Capacitor (a) V_{C1} , (b) V_{C2} , (c) V_{C3} , (d) V_{C4} , (e) V_{C5}

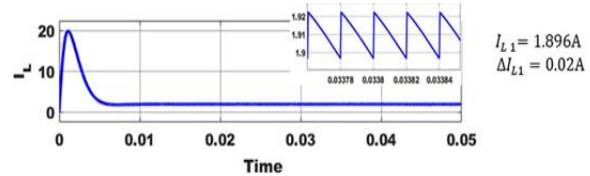


Fig. 10. Current across Inductance (a) i_L

IV. PERFORMANCE ANALYSIS

The efficiency of power equipment at any given load is defined as the ratio of output power to input power. In this study, the relationship between efficiency and output power for a Modified Dual-Switch Boost DC-DC Converter was analyzed under both resistive (R) and resistive-inductive (RL) loading conditions, as illustrated in Fig. 11. The converter achieved peak efficiencies of 93.1% for the R load and 90.4% for the RL load. The efficiency variation across output power levels is moderate, particularly around 100 W. These results indicate that the Modified Dual-Switch Boost Converter is well-suited for medium-power applications.

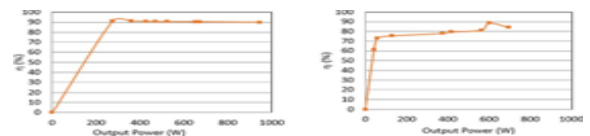


Fig. 11. Efficiency Vs Output Power for (a) R load (b) RL load

Figure 12 illustrates the gain of the Modified Dual-

Switch Boost DC-DC Converter plotted against the duty ratio. It can be observed that the gain rises with an increase in the duty ratio.

The plot of output voltage ripple as a function of duty Ratio

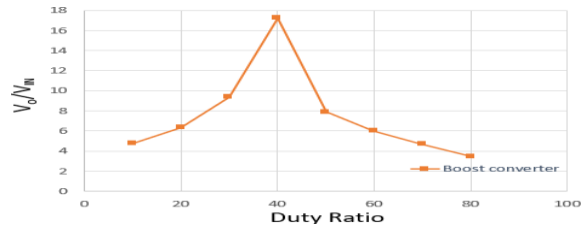


Fig. 12. Voltage gain VS Duty ratio

for Modified Dual-Switch Boost DC-DC Converter is shown in figure 13.

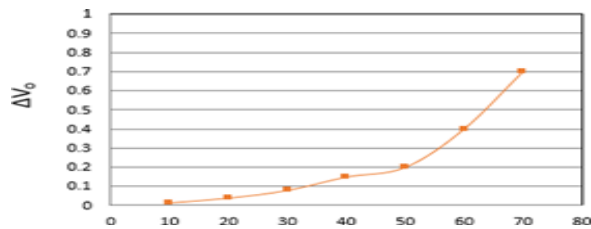


Fig. 13. Output Voltage Ripple VS Duty Ratio

Figure 14 illustrates the output voltage ripple behavior of the modified boost converter with respect to varying switching frequencies. It is observed that the output voltage ripple diminishes as the switching frequency increases.

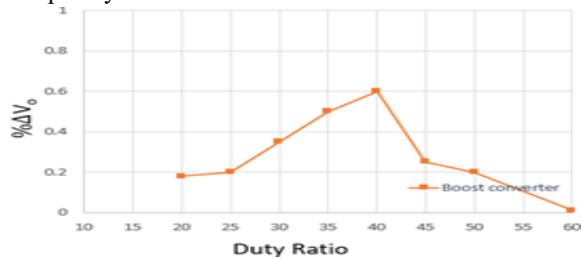


Fig. 14. Output voltage ripple VS frequency

V. COMPARITIVE STUDY

A comparative analysis between the conventional Modified Dual-Switch Boost DC-DC Converter and the proposed enhanced version—both operating under identical conditions with an input voltage of 48V and a switching frequency of 50kHz—is presented in Table 2. The results indicate that, with the duty ratio held constant, the voltage gain

improves significantly from 4.17 to 8.34 in the proposed topology. However, this improvement comes at the cost of increased output voltage and current ripple, which is a trade-off to consider in practical applications.

TABLE II

COMPARISON BETWEEN DUAL-SWITCH BOOST DC-DC CONVERTER& PROPOSED MODIFIED DUAL-SWITCH BOOST DC-DC CONVERTER

Parameters	Dual-Switch Boost Converter	Modified Dual-Switch Boost Converter
No. of Switches	2	2
No. of Inductor	1	1
No. of Diode	4	6
No. of Capacitor	3	5
Voltage Gain	4.16	8.33
Output Voltage	200V	400V
Peak Overshoot of Inductor Current	45A	20A
Voltage stress	100V(50% of V_o)	50V(25% of V_o)

Table 3 provides a detailed comparison of the components used in the proposed Modified Dual-Switch Boost DC-DC Converter against those in other converter designs.

TABLE III

COMPARISON BETWEEN MODIFIED DUAL-SWITCH BOOST DC-DC CONVERTER& OTHER CONVERTERS

Converter	Boost converter in [6]	Boost converter in [7]	Boost converter in [9]	Modified Dual-Switch Boost converter
No. of Switches	2	2	1	2
No. of Diodes	2	2	3	5
No. of Inductors	2	2	3	1
No. of Capacitors	2	2	5	5
Power	50 W	40 W	500 W	100 W
Voltage Gain	$\frac{1-D}{1+D}$	$\frac{2}{1-D}$	$\frac{3-2D}{1-2D}$	$\frac{4}{1-2D}$

VI. EXPERIMENTAL SETUP WITH RESULT

For the purpose of implementing hardware, the input voltage is reduced to 2V and the switching pulses are generated using TMS320F28335 processor. The switch used is MOS-FET IRF3205. Driver circuit is implemented using TLP250H, which is an optocoupler used to isolate and protect the microcontroller from any damage and also to provide

required gating to turn on the switches.

Experimental setup of Modified Dual-Switch Boost DC-DC Converter is shown in Fig. 15. Input 2V DC supply is given from DC source. Switching pulses are taken from TMS320F28335 microcontroller to driver circuit. Thus, an output voltage of 8.6V is obtained from power circuit that is shown in Fig. 16. Output voltage of converter is taken from the DSO oscilloscope.

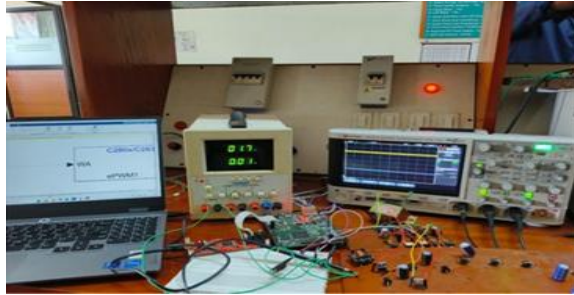


Fig. 15. Experimental Setup

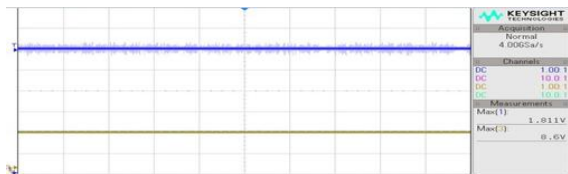


Fig. 16. Output Voltage of Proposed Converter

VII. CONCLUSION

A novel gain-boost converter design with reduced voltage stress on the switching components has been developed and implemented. This topology integrates features of both switched capacitor circuits and voltage multiplier cells. Compared to conventional boost DC-DC converters, the proposed configuration provides a higher voltage gain along with minimized voltage stress on the switches. The converter has been simulated and analyzed, and the results indicate that it achieves an efficiency of 89% at an output power level of 100W. From the analysis it can be seen that modified converter achieves a peak efficiency of 93% for an output power of 100W. The converter was tested with an input voltage of 2 V and was capable of boosting the output to a regulated voltage of 9V, confirming its suitability for high-gain applications. The control and pulse generation were implemented using a TMS320F28335 DSP board, which provided precise PWM gate signals to the switching devices. This

high-performance digital controller ensured accurate duty cycle modulation, fast dynamic response, and stable voltage regulation under varying load conditions. With its combination of high voltage gain, compact design, low component stress, and digital control integration, the proposed converter topology proves to be an excellent power interface solution for fuel cell vehicles, photovoltaic energy systems, and distributed energy resources where high step-up DC conversion is required.

REFERENCES

- [1] M. Veerachary and P. Sen, "Dual-Switch Enhanced Gain Boost DC-DC Converters," in *IEEE Transactions on Industry Applications*, vol. 58, no. 4, pp. 4903-4913, July-Aug. 2022
- [2] A. Kumar et al., "A High Voltage Gain DC-DC Converter with Common Grounding for Fuel Cell Vehicle," in *IEEE Transactions on Vehicular Technology*, 2020
- [3] Yun Zhang, Lei Zhou, Mark Sumner, Ping Wang, Single-switch, wide voltage-gain range, boost DC-DC converter for fuel cell vehicles, *IEEE Transactions on Vehicle Technology*, vol. 67, no. 1, pp. 134-145, Jan. 2018
- [4] Si Chen, Luwei Zhou, Quanming Luo, Wei Gao, Yuqi Wei, Pengju Sun, Xiong Du, Research on topology of the highstep-up boost converter with coupled Inductor, *IEEE Transactions on Power Electronics*, vol. 34, no.11, pp. 10733-10745, Nov. 2019.
- [5] John Joy, Beena M. Varghese, Bos Mathew Jos, Smitha Paulose, Eldhose K. A., "Non-Isolated Enhanced Gain DC-DC Converter," in *Proc. Int. Conf. Smart Control of Electrical and Energy Systems (ICSCC)*, Aug. 2023.
- [6] Aswini Narayanan, Beena M. Varghese, Smitha Poullose, Bos Mathew Jos, "Design and Analysis of PV Integrated Multilevel Inverter for Grid Application," in *Proc. Int. Conf.*, Nov. 2020.
- [7] Bhagyalakshmi P. S., Beena M. Varghese, Bos Mathew Jos, "A Single Switched Capacitor Cell Multilevel Inverter using APOD PWM Technique for Power Grid Application," *Int. J. Eng. Trends Technol. (IJETT)*, vol. 48, no. 4, pp. 205-212, Jun. 2017.